

# Effect of C–H...X interactions (X = O, S, $\pi$ ) in the supramolecular arrangements of 3-ferrocenyl-methoxybenzo[*b*]thiophene isomers †

J. L. Ferreira da Silva,<sup>a</sup> André P. Ferreira,<sup>a</sup> M. Matilde Marques,<sup>a</sup> Shrika G. Harjivan,<sup>a</sup> M. Fátima M. da Piedade<sup>ab</sup> and M. Teresa Duarte<sup>\*a</sup>

Received 19th July 2010, Accepted 4th November 2010

DOI: 10.1039/c0ce00434k

Two regioisomers, 3-ferrocenyl-6-methoxybenzo[*b*]thiophene (IV) and 3-ferrocenyl-4-methoxybenzo[*b*]thiophene (V), were isolated after an acid-catalysed intramolecular electrophilic cyclisation of 1-ferrocenyl-2-[3-(methoxyphenyl)thio]ethanone. This paper analyses the effect of the different positioning of the methoxy group in the benzothiophene ring on the molecular and crystal structures of both molecules. In isomer IV this group is more exposed to interactions with adjacent molecules than in V; thus, while in IV the C<sub>OMe</sub>–H...O<sub>OMe</sub> intermolecular interactions determine the crystal packing, in V the overall assembly results from an interplay of the C<sub>Cp</sub>–H...O<sub>OMe</sub>, C<sub>Cp</sub>–H...S and C<sub>Cp</sub>–H/ $\pi$  interactions. The supramolecular analysis provides an explanation for the spontaneous solid state separation of these regioisomers and their different physical properties, such as their melting points and their ability to interact with supports during chromatographic separations.

## Introduction

The incorporation of organometallic moieties into the structure of known active drugs to improve their therapeutic properties has gained considerable interest in recent years.<sup>1</sup> With the aim of exploring the concept of target-oriented organometallic drugs, we have been investigating the modification by organometallic fragments of the benzo[*b*]thiophene derivative raloxifene (I, Fig. 1), a selective oestrogen receptor modulator used in the prevention of osteoporosis and effective in reducing breast cancer incidence in postmenopausal women at increased risk.<sup>2,3</sup> As part of this strategy, we have synthesized and characterized a series of bio-organometallic benzo[*b*]thiophene derivatives (II, Fig. 1) containing a ferrocenyl unit and several terminal

alkylamino groups, which displayed interesting activities against several tumor cell lines *in vitro*.<sup>4</sup>

A key step in the synthetic sequence leading to the final raloxifene analogues was the acid-catalysed intramolecular electrophilic cyclisation of 1-ferrocenyl-2-[3-(methoxyphenyl)thio]ethanone (III, Fig. 2), which resulted in the formation of two regioisomers, depending on whether the electrophilic attack occurred *para* or *ortho* to the methoxy group. We report herein a comparative characterization of these two regioisomers,

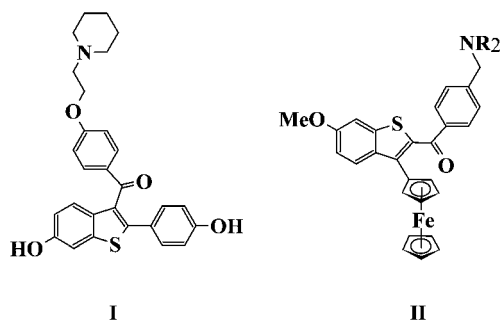


Fig. 1 Structures of raloxifene (I) and the bioorganometallic raloxifene analogues (II) mentioned in the text.

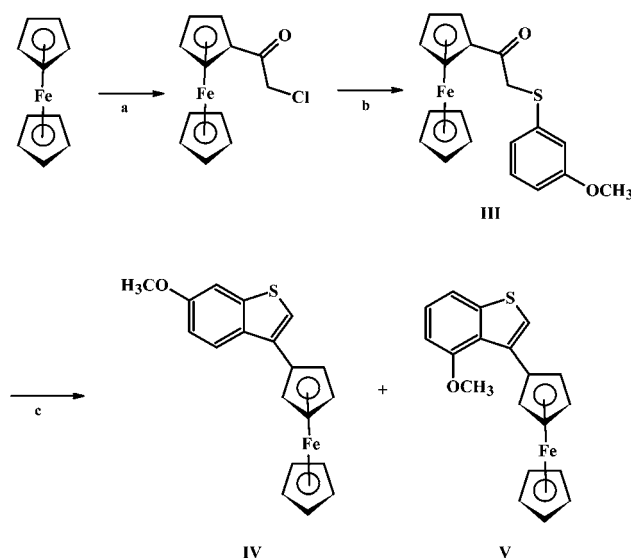


Fig. 2 Synthesis of 1-ferrocenyl-2-[3-(methoxyphenyl)thio]ethanone (III), and acid-catalysed cyclisation of III, leading to the formation of 3-ferrocenyl-6-methoxybenzo[*b*]thiophene (IV) and 3-ferrocenyl-4-methoxybenzo[*b*]thiophene (V). Experimental conditions:<sup>4</sup> (a) chloroacetyl chloride, AlCl<sub>3</sub>, dry CH<sub>2</sub>Cl<sub>2</sub>; (b) 3-methoxybenzenethiol, potassium *tert*-butoxide, diethyl ether; and (c) activated Amberlyst®, *p*-xylene, reflux.

<sup>a</sup>Centro de Química Estrutural, Instituto Superior Técnico, TU Lisbon, Av. Rovisco Pais, 1049-001 Lisboa, Portugal. E-mail: teresa.duarte@ist.utl.pt; Fax: +351-218417246; Tel: +351-218419282

<sup>b</sup>Departamento de Química e Bioquímica, FCUL, Campo Grande, 1749-016 Lisboa, Portugal

† CCDC reference numbers 760582 and 760583. For crystallographic data in CIF or other electronic format see DOI: 10.1039/c0ce00434k

3-ferrocenyl-6-methoxybenzo[*b*]thiophene (**IV**) and 3-ferrocenyl-4-methoxybenzo[*b*]thiophene (**V**), that were obtained using the synthetic pathway outlined in Fig. 2. The major product, isomer **IV**, formed with a regioselectivity of 95%, was presumably favoured over **V** due to the stereochemical constraints associated with ring closure *ortho* to both pre-existing substituents. So far we have prepared the bioorganometallic raloxifene analogues using isomer **IV** as the starting material, but we aim to tune the synthetic conditions toward improving the yield of isomer **V** in order to use it as a starting material for the synthesis of a new family of raloxifene-like compounds.

Crystal design and engineering embraces, as one of its most important issues, the rational design and structural control of molecular packing, which is known to affect and control the physical properties of the materials.<sup>5</sup> In this context, hydrogen bonding is the most robust and directional supramolecular interaction playing a dominant role in molecular aggregation.<sup>6</sup> The weak C–H...X (X = O, S,  $\pi$ ) hydrogen bonds will be brought into play in the study of the different supramolecular assemblies observed in this isomeric organometallic compounds and correlate them with their physical properties.

## Results and discussion

We present and discuss here a comprehensive solid state approach to the influence of supramolecular arrangement in the spontaneous solid state separation of these regioisomers and their physical properties.

The two isomers are easily isolated in the solid state, as their crystalline habits, induced by their intermolecular interactions, are very different: one, 3-ferrocenyl-6-methoxybenzo[*b*]thiophene (**IV**), crystallizes as plates and the other, 3-ferrocenyl-4-methoxybenzo[*b*]thiophene (**V**), as prismatic crystals.

### Molecular and crystal structure

Single crystal X-ray diffraction analysis allowed us to fully characterize both isomers. While isomer **IV** crystallizes in the monoclinic  $P2_1/c$  space group, isomer **V** crystallizes in the triclinic  $P1$  space group with  $Z' = 2$  (Fig. 3 and 4). Selected bond lengths, angles and geometrical parameters are presented in Table 1.

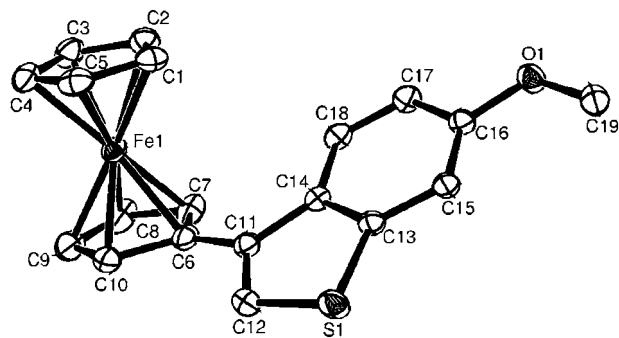


**Fig. 3** ORTEP diagram, drawn with 50% probability ellipsoids, showing the atomic labelling scheme for 3-ferrocenyl-6-methoxybenzo[*b*]thiophene (**IV**).

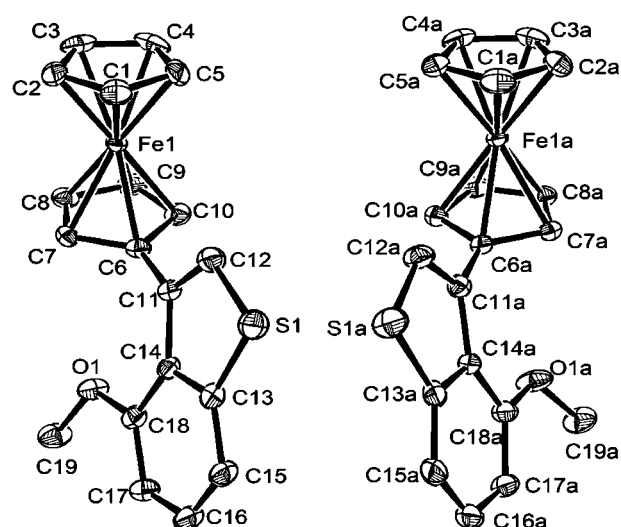


**Fig. 4** ORTEP diagram, drawn with 50% probability ellipsoids, showing the atomic labelling scheme for molecules **1** (left) and **2** (right) of 3-ferrocenyl-4-methoxybenzo[*b*]thiophene (**V**).

Bond lengths and angles of the ferrocenyl groups and the 5-membered thiophene ring are similar in all three molecules and well within the expected values, as judged from extensive analysis of the values included in the CSD.<sup>7,8</sup> The absence of CSD data concerning the full benzo[*b*]thiophene molecule precluded a similar comparison with the results obtained for the 6-membered ring. Nonetheless, its bond lengths and angles are in good agreement with the values obtained for two derivatives of **IV** with potential antitumor properties (Fig. 1, **II**,  $R_2NH$  = pyrrolidine and morpholine) previously published by us<sup>4</sup> and display values comparable to those reported by Ogawa *et al.* for similar benzochalcogenophenes containing ferrocenyl fragments.<sup>9</sup>

The main differences in the geometric parameters of the two compounds lie in the relative values of the angle between the Cp(C6–C10) ring and the benzo[*b*]thiophene moiety ( $29.2^\circ$  in isomer **IV** and  $69.8^\circ$  and  $-67.2^\circ$  in the two molecules of **V**), together with the corresponding values of the torsion angles involving the C(6)–C(11) bond (see Table 1). This major difference, that surely plays a significant role in the selection of crystallization habit, depends mostly on the relative positioning of the methoxy group. In fact, the methoxy substituent, at position 6 of the benzo[*b*]thiophene ring in isomer **IV**, is oriented away from the ferrocenyl group; in contrast, in isomer **V** its presence in position 4 leaves it facing the ferrocenyl group. Moreover, in the asymmetric unit of **V** it is noticeable the existence of a pseudosymmetric  $P1$  crystal structure bearing two enantiomeric molecules (Fig. 5) with the methoxy group oriented alternatively towards each of the Cp *ortho* hydrogen atoms. Their existence could be explained by the formation of two very weak intramolecular  $C_{Cp}\text{--}H\cdots O$  interactions (Fig. 5).

As expected, the conformation of the methoxy moiety is also affected, displaying two different values for the torsion angles C(19)–O(1)–C(18)–C(17), respectively  $6.1^\circ$  in **V-1** and  $-15.6^\circ$  in **V-2**. This is further emphasized when compared with **IV**, where the corresponding torsion angle is close to zero ( $0.4^\circ$ ).

Further indication that the geometry of the two isomers is likely to subsist, at least to some extent, in solution, stems from

**Table 1** Selected bond lengths and angles for compounds **IV** and **V**

	Isomer <b>IV</b>	Isomer <b>V</b> (molecule 1)	Isomer <b>V</b> (molecule 2)
Bonds/Å			
Fe(1)–centroid Cp(C1–C5)	1.647(6)	1.651 (1)	1.650 (2)
Fe(1)–centroid Cp(C6–C10)	1.642(6)	1.644 (1)	1.653 (1)
Average C–C Cp's	1.428 (2)	1.412 (5)	1417 (5)
C(6)–C(11)	1.469 (2)	1.477 (4)	1.477 (4)
S(1)–C(12)	1.729 (1)	1.730 (3)	1.722 (3)
S(1)–C(13)	1.735 (1)	1.739 (3)	1.735 (3)
C(11)–C(12)	1.363 (2)	1.357 (4)	1.352 (4)
C(14)–C(11)	1.454 (2)	1.456 (4)	1.441 (4)
C(14)–C(13)	1.408 (1)	1.405 (4)	1.400 (4)
C(15)–C(13)	1.403 (1)	1.410 (5)	1.388 (5)
C(15)–C(16)	1.384 (1)	1.365 (5)	1.371 (5)
C(16)–C(17)	1.411 (2)	1.396 (4)	1.408 (4)
C(17)–C(18)	1.381 (2)	1.388 (4)	1.380 (4)
C(14)–C(18)	1.412 (2)	1.417 (4)	1.413 (4)
Torsion angles/°			
C(12)–C(11)–C(6)–C(7)	−151.3 (1)	115.6 (4)	−119.1 (3)
C(12)–C(11)–C(6)–C(10)	27.0 (2)	−66.5 (4)	64.8 (4)
C(14)–C(11)–C(6)–C(7)	27.5 (2)	−70.9 (4)	66.2 (4)
C(14)–C(11)–C(6)–C(10)	−154.2 (1)	106.9 (3)	−109.8 (3)
C(19)–O(1)–C(16)–C(15)	0.4 (1)		
C(19)–O(1)–C(18)–C(17)		−6.2 (4)	15.7 (4)
Tilt angle <sup>a</sup>	10.41	−20.07	15.56
Angles between planes/°			
Cp(C6–10)/benzothiophene	29.2 (1)	69.8 (1)	−67.2 (1)

<sup>a</sup> C(1)–Cp(C1–5)<sub>centroid</sub>–Cp(C6–10)<sub>centroid</sub>–C(6).

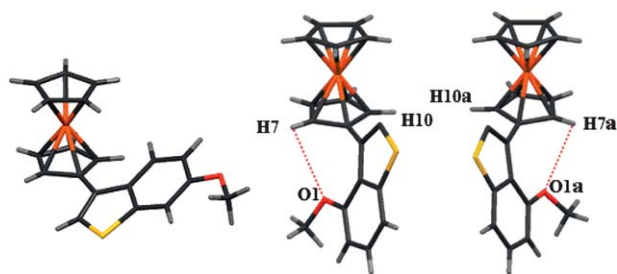


**Fig. 5** Diagrams showing the relative conformations of molecules **IV** (left), **V-1** (centre) and **V-2** (right), displaying the very weak intramolecular  $C_{cp}\text{--}H\cdots O$  hydrogen interactions in isomer **V**: C(7)...O(1), 3.038 Å; H(7)...O(1), 3.041 Å; C(10)–H(10)...O(1), 80.9°; and C(7a)...O(1a), 2.908 Å; H(7a)...O(1a), 2.918 Å; C(7a)–H(7a)...O(1a), 80.1°.

analysis of the NMR spectra. In fact, a comparison of the  $^1H$  and  $^{13}C$  NMR data for isomers **IV**<sup>4</sup> and **V** (this work) in acetone reveals noteworthy downfield shifts of the benzothiophene H12 (0.37 ppm) and particularly C12 (6.6 ppm) in isomer **V**, which presumably reflects positioning of the C12–H12 bond in the deshielding zone of the ferrocenyl substituent. This is consistent with the solid state conformations displayed in Fig. 4.

### Supramolecular arrangement

These two compounds are isomers, therefore display the same molecular functionalities, but crystal structure is completely diverse, a consequence of the different relative positioning of the various functional groups within the molecule. It is possible to identify in these molecules four groups that, by donor–acceptor recognition processes, can interact: the methoxy group, the sulfur atom, the  $\pi$  ring systems and the multiple aromatic C–H bonds.

The strongest acceptor present is, undoubtedly, the methoxy oxygen atom, whose different positioning should, therefore, have an effect on ensuing the intermolecular hydrogen bonds thus determining the supramolecular arrays displayed by both regioisomers.

So it is expected to detect the presence of C–H...O and C–H...S hydrogen bonds, which some authors usually consider too feeble to influence supramolecular arrangements.<sup>10</sup> Moreover, it is also possible to predict, due to the presence of several  $\pi$  aromatic ring systems, the existence of even weaker C–H/ $\pi$  short contacts, the most common intermolecular interactions found in the 3D crystal structures, and that have shown to direct and determine the self-assemblies observed in the two compounds.

C–H/ $\pi$  interaction is defined as a short contact between a soft acid C–H and a soft base  $\pi$ -system, displaying the lower energy values (0.5–2 kcal mol<sup>−1</sup>) of the intermolecular interactions, as opposed to strong hydrogen bonds (hard acid–hard base, 3–7 kcal mol<sup>−1</sup>). However, the cooperative effect of a large number of these interactions makes them very important in the global context of the supramolecular arrangement. They play fundamental roles in stabilizing the conformations of organic molecules, as well as in the crystal packing of organic<sup>10,11</sup> and organometallic compounds.<sup>12,13</sup> All the C–H/ $\pi$  interactions reported in the present work have the hydrogen atom positioned above the  $\pi$  plane, since this contact results from charge transfer from the  $\pi$ -electrons to the anti-bonding orbital of the C–H bond.<sup>14</sup>

Different geometrical parameters have been used to describe this type of interactions.<sup>11</sup> The criteria recently developed by Nishio and co-workers<sup>12</sup> will be adopted in the current manuscript, due to their suitability to the geometry of the type of interactions reported herein (Fig. 6).

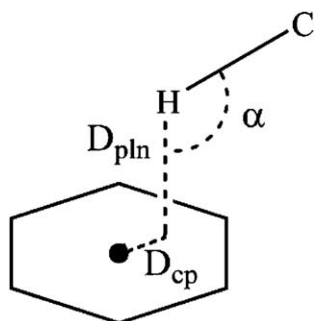


**Fig. 6** Important parameters in a C–H/π interaction (adapted from Nishio and co-workers<sup>12</sup>).  $D_{\text{pln}}$ —distance from the H atom to the plane of the  $\pi$  ring system,  $D_{\text{cp}}$ —distance between the projection of the hydrogen atom on the ring plane and the  $\pi$  system centroid, and  $\alpha$ —angle between the C–H bond and the projection of the hydrogen atom on the ring plane.

**Isomer IV.** In isomer IV, the methoxy oxygen is free to establish a relatively strong intermolecular  $\text{C}_{\text{OMe}}\text{--H}\cdots\text{O}$  hydrogen bond with a methoxy hydrogen of the neighbouring molecule. These interactions make up the backbone of the final supramolecular array, forming a C(3) synthon, a zigzag chain in plane  $ab$ , that grows along the  $b$ -axis (Fig. 7). This molecular arrangement is favoured by the relative positioning of the Cp and its benzothiophene substituent, a  $\sim 30^\circ$  dihedral angle.

A pair of these chain molecules (Fig. 8, **A** and **B**) interacts with two other molecules (**C** and **D**) by four C–H $\cdots$ S contacts, forming two  $R^2_2(8)$  synthons. It should be noticed that the 5 member moiety of the benzothiophene ring of molecule **A** is also involved in a C–H/π interaction with the C(5)–H(5) bond of a Cp ring of molecule **D**.

The final 3D supramolecular arrangement for this isomer is attained by a network of C–H/π interactions, as previously

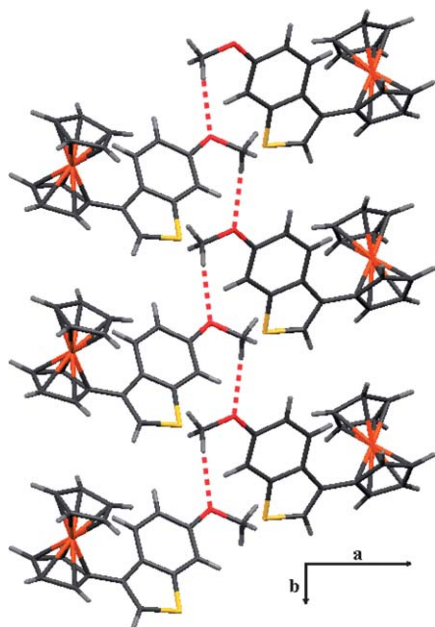


**Fig. 7** Zigzag chains of molecule IV (view along  $c$ ) based on  $\text{C}_{\text{OMe}}\text{--H}\cdots\text{O}$  hydrogen bonds: C(19) $\cdots$ O(1) = 3.507 Å; H(19c) $\cdots$ O(1) = 2.566 Å; C(19)–H(19a) $\cdots$ O(1) =  $162.5^\circ$ .

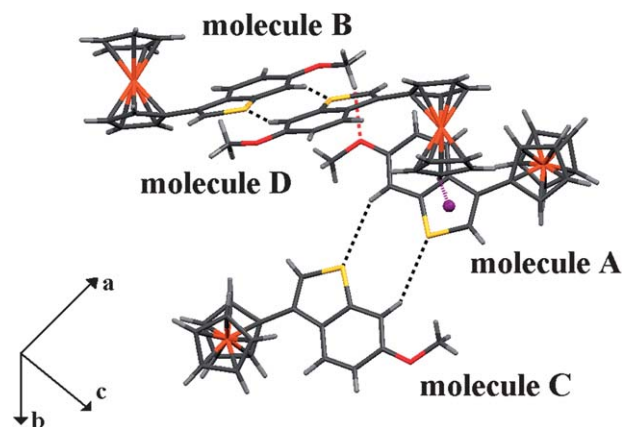


**Fig. 8** View of the crystal packing in isomer IV showing in detail the  $\text{C}_{\text{benzothiophene}}\text{--H}\cdots\text{S}$  (C(15) $\cdots$ S(1) = 3.874 Å; H(15) $\cdots$ S(1) = 3.041 Å; C(15)–H(15) $\cdots$ S(1) =  $146.6^\circ$ , in black) and the  $\text{C}_{\text{Cp}}\text{--H}/\pi$  ( $D_{\text{pln}}$  = 2.637 Å,  $D_{\text{cp}}$  = 0.385 Å,  $\alpha$  =  $159.7^\circ$ , in purple) interactions.

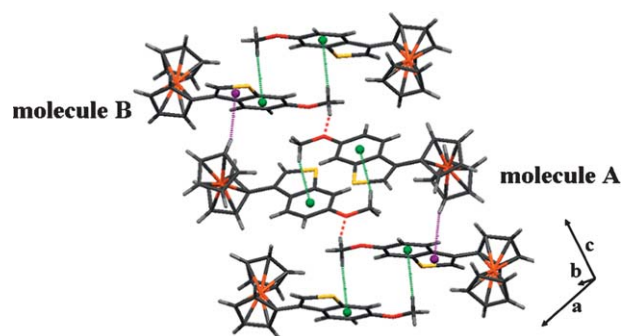


**Fig. 9** View of the crystal packing showing in detail the  $\text{C}_{\text{OMe}}\text{--H}/\pi$  ( $D_{\text{pln}}$  = 2.629 Å,  $D_{\text{cp}}$  = 0.341 Å,  $\alpha$  =  $139.2^\circ$ , in green) and the  $\text{C}_{\text{Cp}}\text{--H}/\pi$  interactions in isomer IV.

mentioned. Fig. 9 shows that the same pair of molecules **A** and **B** from Fig. 8 can additionally pair off with two other molecules *via*  $\text{C}_{\text{OMe}}\text{--H}/\pi$  short contacts<sup>11</sup> involving the  $\pi$  electron system of the 6-membered part of the benzothiophene ring (represented in green in Fig. 9).

This pairing is favoured by the mobility of the benzothiophene moiety, enabling the alignment of the two ring systems. This supramolecular array is again reinforced by another aromatic  $\text{C}_{\text{Cp}}\text{--H}/\pi$  short contact<sup>14</sup> between the C(5)–H(5) bond of a Cp ring and the  $\pi$  electron system of the 5-membered segment of the benzothiophene ring (represented in purple in Fig. 9). All geometrical parameters found for the C–H/π interactions are within the range usually reported for this type of short contacts.<sup>11,12</sup>

**Isomer V.** Again in this isomer it is expected that C–H $\cdots$ O hydrogen bonds will be the prevalent interactions in the supramolecular arrangement. In fact these contacts are observed between the methoxy oxygen of a type 1 molecule and a hydrogen of a substituted Cp ring from a type 2 molecule (Fig. 10). However, the methoxy oxygen of type 2 molecules is not involved in any kind of short contacts with other molecules.



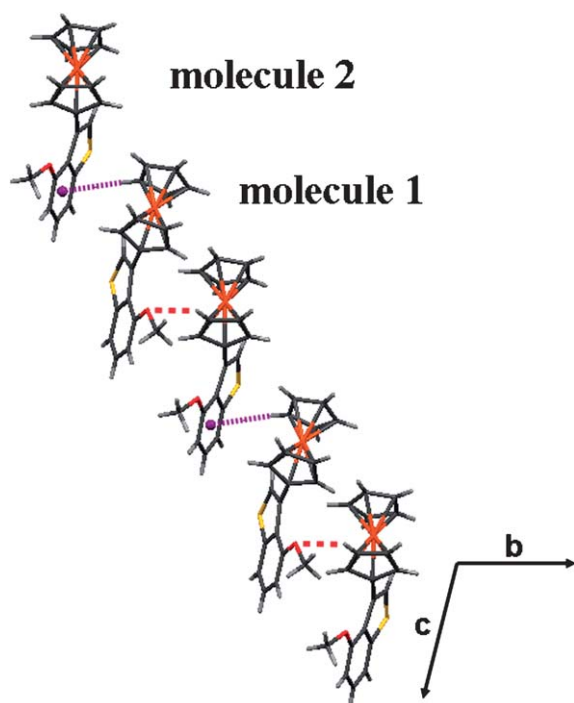


**Fig. 10** View of the chain formed by the two types of isomer **V** molecules using  $C_{Cp}-H...O$  hydrogen bonds ( $C(8a)...O(1) = 3.543 \text{ \AA}$ ;  $H(8a)...O(1) = 2.691 \text{ \AA}$ ;  $C(8a)-H(8a)...O(1) = 149.6^\circ$ , in red) and aromatic  $C_{Cp}-H/\pi$  interactions ( $D_{pln} = 2.724 \text{ \AA}$ ,  $D_{cp} = 1.111 \text{ \AA}$ ,  $\alpha = 161.1^\circ$ , in purple) (view along axis *a*).

In isomer **V** the substituted Cp and the benzothiophene adopt a relative positioning close to perpendicularity, with angles of  $\sim 70^\circ$ . This arrangement leaves a  $C_{Cp}-H$  bond of a type **1** molecule in the correct positioning toward a 6-membered ring of a type **2** molecule to allow the formation of an aromatic  $C_{Cp}-H/\pi$  interaction. The combination of these two kinds of interactions creates an alternated linear chain of molecules **1** and **2** (Fig. 10).

This 1D arrangement leaves the 6-membered ring of the benzothiophenes of type **2** molecules in a geometrically favoured position to create a supramolecular array by establishing  $C_{Cp}-H...S$  interactions and  $C_{Cp}-H/\pi$  contacts with molecules from neighbouring parallel chains. These interactions lead to a final 2D sheet, as can be seen in Fig. 11. Again, all geometrical parameters found for these two types of interactions are within the range usually reported.<sup>10–12</sup>

It is possible to visualize from this figure that this network of intermolecular interactions is formed by alternated lines: one of  $C_{Cp}-H...S + C_{Cp}-H...O$  interactions and another formed only by  $C_{Cp}-H/\pi$  contacts. A feature that emerges from Fig. 11 is that type **1** molecules are always in the acceptor's end of  $C_{Cp}-H...S$  interactions, while type **2** molecules use their 6-membered ring as the acceptor for  $C_{Cp}-H/\pi$  contacts. This situation can force the molecules to rotate around the  $C(6)-C(11)$  bond, making the benzothiophene to lean on towards the side of the donor group of each one of these interactions and create the two different unequivalent geometries observed for the molecules in the unit cell of this compound. This figure also confirms that only half of the methoxy groups participate in the  $C_{Cp}-H...O$  interactions, a situation that probably arises from the different values of

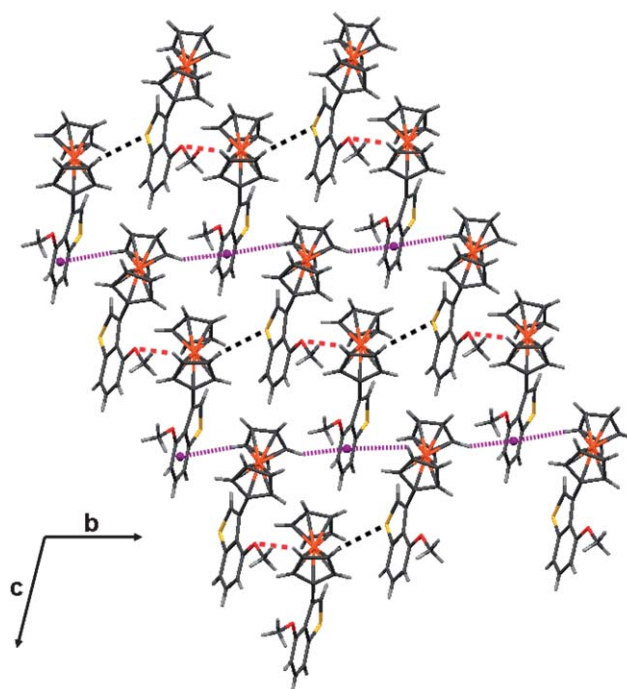


**Fig. 11** Assembly of chains from isomer **V** (view along axis *a*), via  $C_{Cp}-H...S$  interactions ( $C(9a)...S(1) = 3.795 \text{ \AA}$ ;  $H(9a)...S(1) = 3.009 \text{ \AA}$ ;  $C(9a)-H(9a)...S(1) = 141.1^\circ$ ) and  $C_{Cp}-H/\pi$  contacts between parallel chains ( $D_{pln} = 2.689 \text{ \AA}$ ,  $D_{cp} = 0.920 \text{ \AA}$ ,  $\alpha = 159.4^\circ$ ).

torsion angles around the  $C(6)-C(11)$  bond, that leave the methoxy oxygen of type **2** molecule too far away from any hydrogen atom to form  $C-H...O$  hydrogen bonds.

#### Effect of the interactions on the properties of the isomers

It is well known that the nature and strength of the intermolecular interactions in the solid state play an important role on the physical properties of chemical compounds. In the case of isomers **IV** and **V** this effect, visible in their spontaneous resolution in the solid state, is also noticeable on their relative affinities for chromatographic polar support media, thus allowing their separation. The two isomers were separated by flash chromatography (see Synthetic procedures) on silica, by eluting with methylene chloride/*n*-hexane (1/4). Before applying this technique, the separation was tested using the same eluting solution on silica thin layer chromatography plates. This test allowed the calculation of the corresponding retention factors ( $R_f$ ):<sup>15</sup> 0.67 for isomer **IV** and 0.73 for isomer **V**. These values indicate that **IV** has a higher affinity for the polar silica support material. The observed difference can be explained by the relative steric hindrance of the methoxy group of both molecules: in compound **IV**, the methoxy group in position 6 of the benzothiophene ring is located in a more exterior situation, increasing its availability to interact with the polar support, resulting in a smaller  $R_f$  value. In compound **V**, in contrast, when bonded in position 4, it achieves a more sheltered situation, adopting a geometry in which this polar group is turned towards the Cp ring, making this interaction more difficult and allowing an efficient separation of the isomers.

The observed difference in the melting point values (105–107 °C for **IV** and 87–89 °C for **V**), a measure of the relative lattice energy of these solids, can also be explained by the diverse supramolecular arrangements observed. The involvement of all methoxy groups in intermolecular C–H...O contacts in **IV**, as opposed to what is observed in **V**, where only half of them are being used, further enhanced by their participation in very weak intramolecular interactions, justifies the lower melting point value measured for isomer **V**.

## Experimental section

### General considerations

All commercially available reagents were acquired from Sigma-Aldrich Química, S.A. (Madrid, Spain). Melting temperatures were measured with a Leica Galen III hot stage apparatus and are uncorrected. <sup>1</sup>H NMR spectra were recorded in acetone-*d*<sub>6</sub>, on a Bruker Avance III 400 spectrometer, operating at 400 MHz. <sup>13</sup>C NMR spectra were recorded on the same instrument, operating at 100.62 MHz. Chemical shifts are reported in ppm downfield from tetramethylsilane and coupling constants (*J*) are reported in Hz; the subscripts *ortho* and *meta* refer to *ortho* and *meta* couplings, and the Ar and Fc abbreviations represent the benzothiophene and ferrocene systems, respectively. Resonance assignments were based on the analysis of coupling patterns, including the <sup>13</sup>C–<sup>1</sup>H coupling profiles obtained in heteronuclear bidimensional HMQC and HMBC experiments, performed with

standard pulse programs. The high resolution mass spectrum (HRMS) of compound **V** was recorded on a Finnigan FT/MS 2001-DT spectrometer.

### Synthetic procedures

Briefly, the synthetic procedure involved refluxing a 0.3 M solution of **III** in *p*-xylene with 10% HCl-activated Amberlyst resin for 4 h, followed by filtration over celite, solvent evaporation and separation of the products using flash chromatography on silica, by eluting with methylene chloride/*n*-hexane (1/4). The benzo[*b*]thiophene derivatives **IV** (*R*<sub>f</sub> 0.67; mp 105–107 °C; 72%) and **V** (*R*<sub>f</sub> 0.73; mp 87–89 °C; 4%) were isolated and recovered as orange crystalline materials. The spectral characterization (IR, <sup>1</sup>H and <sup>13</sup>C NMR, MS) of isomer **IV** has been described.<sup>4</sup>

**3-Ferrocenyl-4-methoxybenzo[*b*]thiophene (V).** <sup>1</sup>H NMR (acetone-*d*<sub>6</sub>) δ 7.78 (1H, s, Ar-*H*2), 7.50 (1H, dd, *J*<sub>ortho</sub> 8.0, *J*<sub>meta</sub> 0.4, Ar-*H*7), 7.30 (1H, t, *J*<sub>ortho</sub> 8.0, Ar-*H*6), 6.88 (1H, d, *J*<sub>ortho</sub> 8.0, Ar-*H*5), 4.65 (2H, t, *J* 2.0, Fc-*H*2 + *H*5 or Fc-*H*3 + *H*4), 4.26 (2H, t, *J* 2.0, Fc-*H*3 + *H*4 or Fc-*H*2 + *H*5), 4.17 (5H, s, Fc-*H*1'–*H*5'), 3.83 (3H, s, CH<sub>3</sub>O). <sup>13</sup>C NMR (acetone-*d*<sub>6</sub>) δ 157.9 (ArC4), 144.1 (ArC7a), 136.4 (ArC3), 129.8 (ArC3a), 126.8 (ArC6), 125.3 (ArC2), 116.8 (ArC7), 106.8 (ArC5), 85.6 (Fc-C1), 72.7 (Fc-C3 + C4 or Fc-C2 + C5), 70.8 (Fc-C1'–C5'), 68.6 (Fc-C3 + C4 or Fc-C2 + C5), 56.0 (CH<sub>3</sub>O). HRMS calcd for C<sub>19</sub>H<sub>16</sub>O<sup>56</sup>Fe<sup>32</sup>S: 348.02657. Found: 348.02612.

**Table 2** Crystal and structure refinement for compounds **IV** and **V**

	<b>IV</b>	<b>V</b>
Chem. formula	C <sub>19</sub> H <sub>16</sub> Fe <sub>1</sub> O <sub>1</sub> S <sub>1</sub>	C <sub>19</sub> H <sub>16</sub> Fe <sub>1</sub> O <sub>1</sub> S <sub>1</sub>
Mol. wt	348.23	348.23
Temperature/K	150(2)	150(2)
Wavelength/Å	0.71073	0.71073
Color/shape	Orange/plate	Orange/prism
Cryst size/mm	0.20 × 0.10 × 0.06	0.30 × 0.20 × 0.16
Cryst. syst.	Monoclinic	Triclinic
Space group	<i>P</i> 2 <sub>1</sub> / <i>c</i>	<i>P</i> 1
<i>a</i> /Å	16.783(2)	7.5490(10)
<i>b</i> /Å	7.5603(11)	9.7340(13)
<i>c</i> /Å	12.1864(17)	11.3500(16)
α/°	—	96.452(8)
β/°	100.689(8)	103.358(7)
γ/°	—	110.027(7)
<i>V</i> /Å <sup>3</sup>	1519.4(4)	745.47(18)
<i>Z</i>	4	2
ρ <sub>calcd</sub> /g cm <sup>−3</sup>	1.522	1.547
Absorption coefficient/mm <sup>−1</sup>	1.128	1.149
<i>F</i> <sub>000</sub>	760	358
θ Range/°	2.47 to 37.40	1.89 to 30.60
Data collected ( <i>h,k,l</i> )	±28, −12 to 11, ±20	−7 to 10, ±13, −16 to 15
Reflections collected/unique	32463/7485	11243/7152
<i>R</i> <sub>(int)</sub>	0.0429	0.0349
Completeness to θ max (%)	98.7	99.5
Max and min transmission	0.9354 and 0.8059	0.8375 and 0.7244
Refinement method	Full-matrix least-squares on <i>F</i> <sup>2</sup>	Full-matrix least-squares on <i>F</i> <sup>2</sup>
Data/restraints/parameters	7845/0/263	7152/3/397
Goodness-of-fit on <i>F</i> <sup>2</sup>	1.009	1.070
Final <i>R</i> indices [ <i>I</i> > 2σ( <i>I</i> )]	<i>R</i> <sub>1</sub> = 0.0362, <i>wR</i> <sub>2</sub> = 0.0843	<i>R</i> <sub>1</sub> = 0.0341, <i>wR</i> <sub>2</sub> = 0.0828
<i>R</i> indices (all data)	<i>R</i> <sub>1</sub> = 0.0565, <i>wR</i> <sub>2</sub> = 0.0935	<i>R</i> <sub>1</sub> = 0.0368, <i>wR</i> <sub>2</sub> = 0.0943
Absolute structure parameter	—	0.004(12)
Largest diff. peak and hole/e Å <sup>−3</sup>	0.614 and −0.338	0.612 and −0.334

## X-Ray crystallographic analysis

X-Ray crystallographic data for compounds **IV** and **V** were collected from crystals using an area detector diffractometer (Bruker AXS-KAPPA APEX II) equipped with an Oxford Cryosystem open-flow nitrogen cryostat at 150 K and graphite-monochromated Mo K $\alpha$  ( $\lambda = 0.71073$  Å) radiation. Cell parameters were retrieved using Bruker SMART software and refined with Bruker SAINT<sup>16</sup> on all observed reflections. Absorption corrections were applied using SADABS.<sup>17</sup> The structures were solved by direct methods using SIR 97<sup>18</sup> and refined with full-matrix least-squares refinement against  $F^2$  using SHELXL-97.<sup>19</sup> All the programs are included in the WinGX package (version 1.70.01).<sup>20</sup> All non-hydrogen atoms were refined anisotropically, and the hydrogen atoms were inserted in idealized positions, riding on the parent C atom, except for the methoxy hydrogens, whose orientation was refined from electron density, allowing the refinement of both O–C torsion angles and C–H distances. Drawings were made with ORTEP-3 for Windows.<sup>21</sup> Intramolecular and intermolecular interactions were analysed using Mercury 1.4.2 (Build 2).<sup>22</sup> Crystals had good quality and diffracting power, presenting low  $R_{\text{int}}$  values (0.0429 for **IV** and 0.0349 for **V**) that allowed low  $R$  values ( $R_1$  all = 0.0565 and  $R_1$  obs = 0.0362 for **IV** and  $R_1$  all = 0.0368 and  $R_1$  obs = 0.0341 for **V**). The structures were, therefore, unequivocally determined and are in agreement with the remaining spectral characterization data for **IV**<sup>4</sup> and **V** (this work). Relevant details of the X-ray data analysis are displayed in Table 2.

## Conclusion

In terms of molecular structures the two ferrocenyl-benzo[*b*]-thiophene isomers discussed in this work diverge essentially in the relative positioning of the substituted ferrocenyl Cp and the benzo[*b*]thiophene moiety. In 3-ferrocenyl-6-methoxy-benzo[*b*]thiophene (isomer **IV**) these two groups form an angle of 29.2°, while in both molecules of 3-ferrocenyl-4-methoxy-benzo[*b*]thiophene (isomer **V**) these angles are 69.8° and –67.2°.

The geometry of the molecules plays an important role in their supramolecular arrangements.

Due to the greater exposure of the methoxy group, isomer **IV** forms zigzag chains using C<sub>OMe</sub>–H...O hydrogen bonds; a pair of molecules, one from each side of the chain, also interact by weaker C<sub>Bz</sub>–H...S contacts. This combination of interactions leaves a large number of planar benzo[*b*]thiophene  $\pi$  systems in the correct positioning to form a 3D supramolecular arrangement by way of C<sub>OMe</sub>–H/ $\pi$  contacts, reinforced by aromatic C<sub>Cp</sub>–H/ $\pi$  short contacts. This type of interactions, although very weak, plays an important role in the definition of the final 3D array of this compound because of the cooperative effect of such a large number of contacts.

In isomer **V** the self-organization of the molecules is dominated by the formation of chains alternating C<sub>Cp</sub>–H...O hydrogen bonds and weaker C<sub>Cp</sub>–H/ $\pi$  contacts; as a result of the near perpendicularity of the ferrocenyl and benzo[*b*]thiophene groups, this chains form a parallel array using C–H...S interactions, reinforced by weaker C–H/ $\pi$  contacts. The different role played on the interactions involved in the formation of this supramolecular structure by the two nonequivalent molecules in

the asymmetric unit of this compound can account for the dissimilar molecular geometries that they present.

The analysis of the intermolecular interactions confirms that, when a considerable number of aromatic rings are present in the molecular structure, the weak C–H/ $\pi$  interactions can play a key role in the definition of the supramolecular array, a feature already reported for a large number of organic and organometallic species.

This study reinforces the known relationship between the physical properties of chemical compounds and the nature and strength of the intermolecular interactions in the solid state.

## Acknowledgements

We thank Conceição Oliveira for obtaining the HRMS of isomer **V**. Thanks are also due to the Portuguese NMR Network (IST-UTL Center) and the Portuguese MS Network (IST-UTL Center) for providing access to the facilities. This work was supported in part by a research grant from Fundação para a Ciência e a Tecnologia (FCT), Portugal (PTDC/QUI/67522/2006) and by a postdoctoral fellowship from FCT to APF (SFRH/BPD/21014/2004).

## References and notes

- G. Jaouen, S. Top and A. Vessières, in *Bioorganometallics: Biomolecules, Labeling, Medicine*, ed. G. Jaouen, Wiley-VCH, Weinheim, 2006, ch. 3, p. 65–95.
- V. G. Vogel, J. P. Costantino, D. L. Wickerham, W. M. Cronin, R. S. Cecchini, J. N. Atkins, T. B. Bevers, L. Fehrenbacher, E. R. Pajon, Jr, J. L. Wade, III, A. Robidoux, R. G. Margolese, J. James, S. M. Lippman, C. D. Runowicz, P. A. Ganz, S. E. Reis, W. McCaskill-Stevens, L. G. Ford, V. C. Jordan and N. Wolmark, For the National Surgical Adjuvant Breast and Bowel Project (NSABP), *JAMA, J. Am. Med. Assoc.*, 2006, **295**, 2727–2741.
- V. G. Vogel, J. P. Costantino, D. L. Wickerham, W. M. Cronin, R. S. Cecchini, J. N. Atkins, T. B. Bevers, L. Fehrenbacher, E. R. Pajon, J. L. Wade, III, A. Robidoux, R. G. Margolese, J. James, C. D. Runowicz, P. A. Ganz, S. E. Reis, W. McCaskill-Stevens, L. G. Ford, V. G. Jordan and N. Wolmark, For the National Surgical Adjuvant Breast and Bowel Project, *Cancer Prev. Res.*, 2010, **3**, 696–706.
- A. P. Ferreira, J. L. Ferreira da Silva, M. T. Duarte, M. F. Minas da Piedade, M. P. Robalo, S. G. Harjivan, C. Marzano, V. Gandin and M. M. Marques, *Organometallics*, 2009, **28**, 5412–5423.
- (a) *Engineering of Crystalline Materials Properties*, ed. J. J. Novoa, D. Braga and L. Addadi, Springer, Dordrecht, The Netherlands, 2008; (b) B. Moulton and M. J. Zaworotko, *Chem. Rev.*, 2001, **101**, 1629–1658.
- (a) G. R. Desiraju, *The Crystal as a Supramolecular Entity*, John Wiley & Sons, Chichester, 1996; (b) D. Braga and F. Grepioni, *Kirk-Othmer Encyclopedia of Chemical Technology*, John Wiley, New York, 5th edn, 2004, vol. 8, p. 65.
- F. H. Allen, O. Kennard, D. G. Watson, L. Brammer, A. G. Orpen and R. Taylor, *J. Chem. Soc., Perkin Trans. 2*, 1987, S1–S19.
- A. G. Orpen, L. Brammer, F. H. Allen, O. Kennard, D. G. Watson and R. Taylor, *J. Chem. Soc., Dalton Trans.*, 1989, S1–S83.
- (a) S. Ogawa, K. Kikuta, H. Muraoka, F. Saito and R. Sato, *Tetrahedron Lett.*, 2006, **47**, 2887–2891; (b) S. Ogawa, H. Muraoka, K. Kikuta, F. Saito and R. Sato, *J. Organomet. Chem.*, 2007, **692**, 60–69.
- G. R. Desiraju and T. Steiner, in *The Weak Hydrogen Bond in Structural Chemistry and Biology*, ed. I. U. C. R., Oxford University Press, Oxford, 1999, p. 231.
- (a) M. Nishio, *CrystEngComm*, 2004, **6**, 130–158; (b) Ref. 9, pp. 122–201 and references cited therein.
- M. Nishio, Y. Umezawa, K. Honda, S. Tsuboyama and H. Suezawa, *CrystEngComm*, 2009, **11**, 1757–1788.
- D. Braga, F. Grepioni and E. Tedesco, *Organometallics*, 1998, **17**, 2669–2672.
- Y. Umezawa, S. Tsuboyama, K. Honda, J. Uzawa and M. Nishio, *Bull. Chem. Soc. Jpn.*, 1998, **71**, 1207–1213.

- 15  $R_f$  (Retardation or retention factor): ratio between the migration distance of the solute and the migration distance of the eluent front in chromatography.
- 16 SMART and SAINT, *Area Detector Control and Integration Software*, Bruker AXS, Madison, WI, USA, 2004.
- 17 SADABS: G. M. Sheldrick, *Program for Empirical Absorption Correction of Area Detectors (Version 2.10)*, University of Göttingen, Germany, 2004.
- 18 A. Altomare, M. C. Burla, M. Camalli, G. L. Cascarano, C. Giacovazzo, A. Guagliardi, A. G. G. Moliterni, G. Polidori and R. Spagna, *J. Appl. Crystallogr.*, 1999, **32**, 115–119.
- 19 G. M. Sheldrick, *SHELXL-97, a Computer Program for the Refinement of Crystal Structures*, University of Göttingen, Göttingen, Germany, 1997.
- 20 L. J. Farrugia, WinGX (v1.70.01), *J. Appl. Crystallogr.*, 1999, **32**, 837–838.
- 21 L. J. Farrugia, ORTEP-3 for Windows (v1.076), based on ORTEP-III (v1.03) by C. K. Johnson, and M. N. Burnett, *J. Appl. Crystallogr.*, 1997, **30**, 565.
- 22 I. J. Bruno, J. C. Cole, P. R. Edgington, M. Kessler, C. F. MacRae, P. McCabe, J. Pearson and R. Taylor, *Acta Crystallogr.*, 2002, **B58**, 389–397.